

Supporting Materials

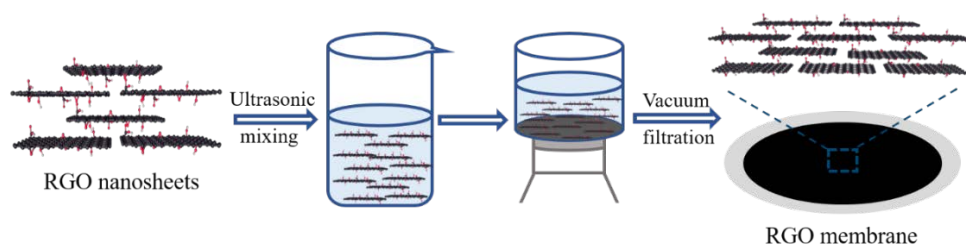


Fig. S1 Illustration of the preparation process of RGO membrane.

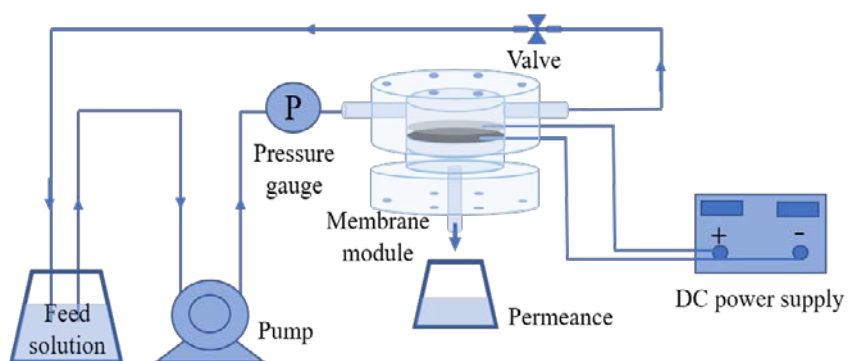


Fig. S2 Schematic diagram of lab-scale cross-flow filtration set-up.

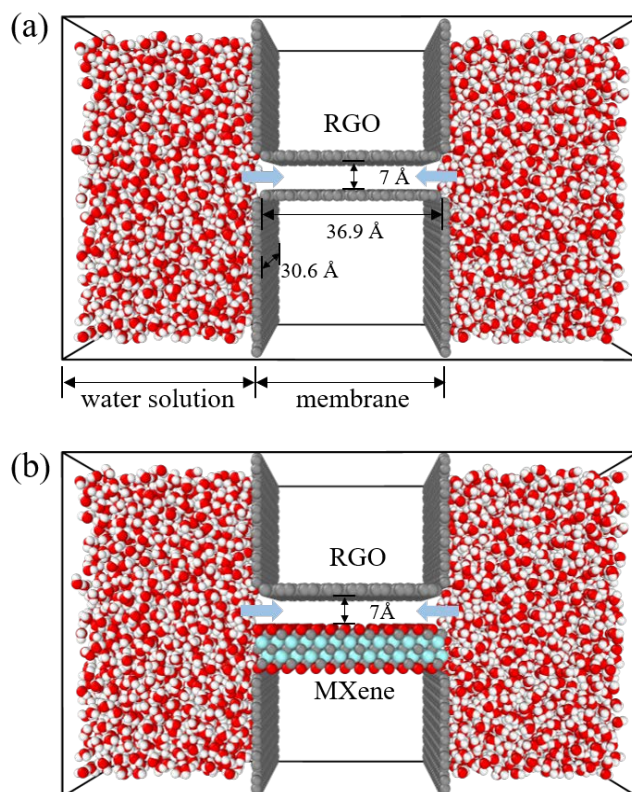


Fig. S3 Cubic chart of the simulation configuration: (a) RGO-RGO channel; (b) RGO-MXene channel. The simulation box is $102 \times 39.5 \times 60 \text{ \AA}^3$. The Ti, C, O and H atoms are shown in grey, blue, red and white spheres, respectively.

Table S1 Force field parameters (Xu et al., 2016; Xu et al., 2018).

Atom	Mass	ϵ (kcal/mol)	σ (nm)	q (e)
C (C-C)	12.011	0.066	3.500	-0.740
Ti-inner	47.867	0.609	1.956	1.040
Ti-outer	47.867	0.609	1.956	1.040
O (Ti-OH)	15.999	0.155	3.166	-0.640
C (C-Ti)	12.011	0.105	3.851	0.000
H (H ₂ O)	15.999	0.155	3.166	-0.848
H (H ₂ O)	1.008	0.000	0.000	0.424

Water contact angle test

First, the RGO-MXene membrane was prepared by the vacuum filtration of RGO and MXene mixture on polyvinylidene fluoride substrate. Then the RGO-MXene membrane was fixed on the sample stage of the optical contact angle tester. Final, a water droplet was dropped on the surface of the RGO-MXene membrane, then photographed when the water droplet just contacted the RGO-MXene membrane surface. The water contact angle was determined by the semicircle

analysis. The test method for the contact angle of RGO membrane is the same as that of RGO-MXene membrane.

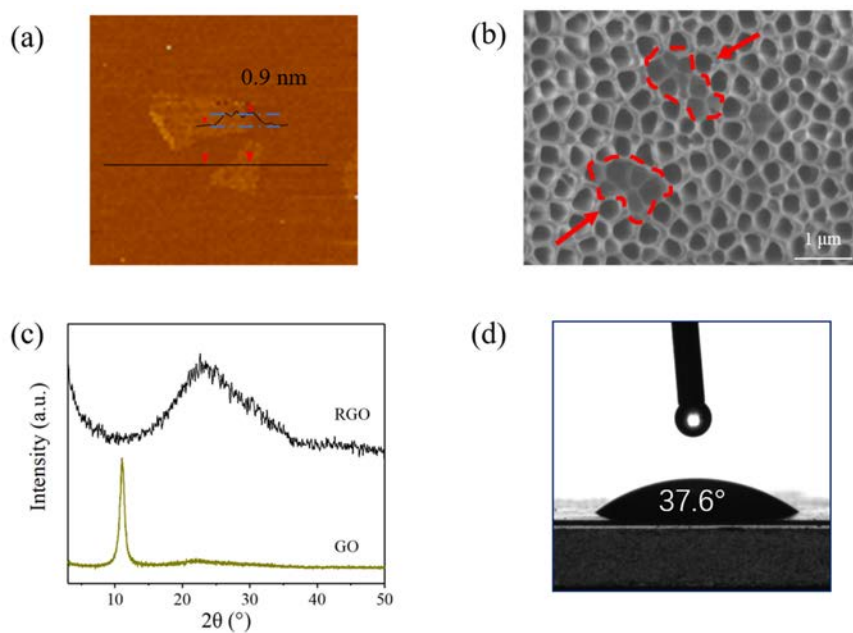


Fig. S4 (a) AFM image of RGO nanosheets; (b) SEM image of RGO nanosheets on an anodic aluminum oxide (AAO) template; (c) XRD patterns of GO and RGO; (d) Water contact angle of GO.

Table S2 Functional group contents obtained from curve fittings in XPS C1s spectra (at.%).

Material	C-C	C=C	C-O/ C-O-C	C=O/ O-C=O	π - π^* shack-up
GO	32.98	13.17	42.81	11.04	0.00
RGO	21.52	64.69	4.18	7.48	2.13

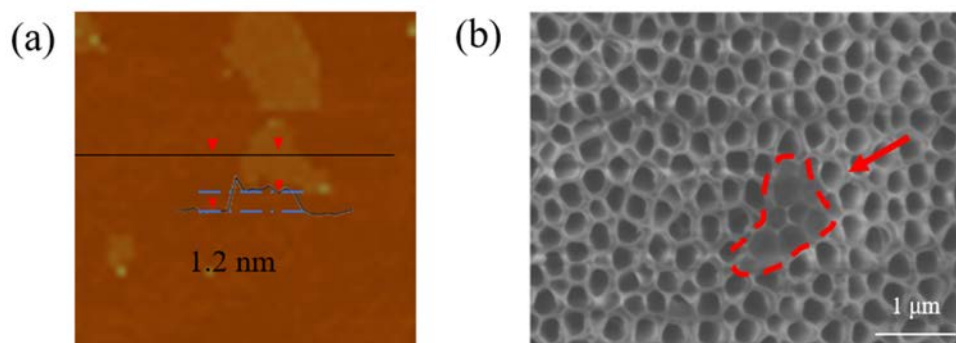


Fig. S5 (a) AFM image of MXene nanosheets; (b) SEM image of MXene nanosheet (Based on an AAO template).

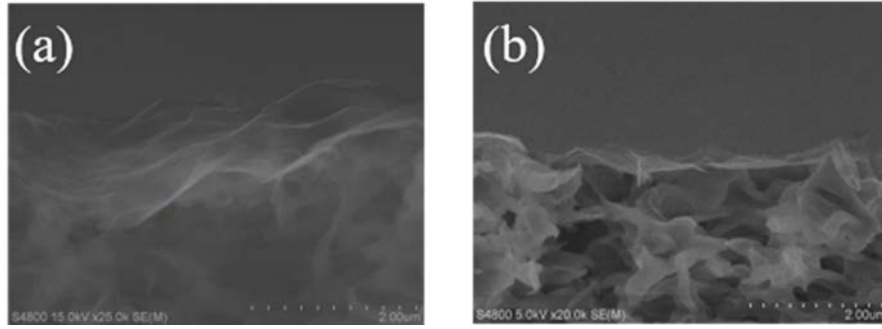


Fig. S6 Cross-sectional SEM images of membranes: (a) RGO membrane; (b) RGO-MXene membrane.

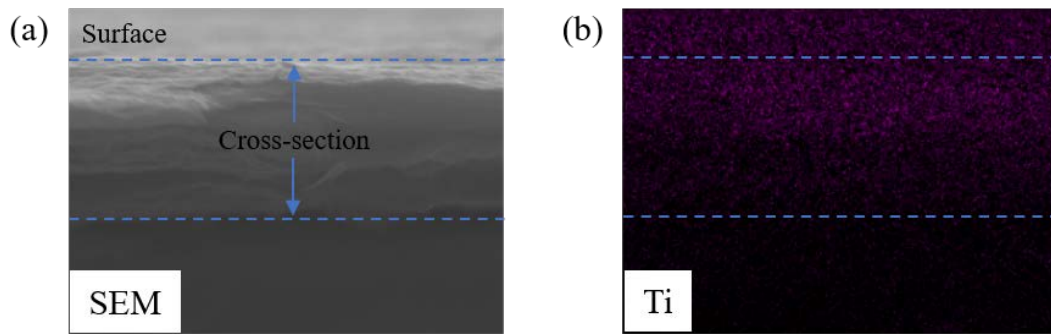


Fig. S7 EDS mapping of the cross-section of RGO-MXene membrane: (a) Cross-section view of RGO-MXene membrane; (b) Distribution of Ti in the cross-section of the RGO-MXene membrane. (For clearly observing the EDS mapping of the cross section of the membrane, we prepared the RGO-MXene membrane with a large RGO-MXene loading mass).

Hagen-Poiseuille equation (Nair et al., 2012):

$$J \approx \delta^3 \left(\frac{1}{12\eta} \right) \left(\frac{1}{L} \right) \left(\frac{\Delta P}{l} \right) \rho \quad , \quad (\text{S1})$$

where J is the water permeance; δ is the interlayer spacing of membrane; η is the viscosity of water at 20°C; L is the lateral width of the nanosheets; Δp is the transmembrane pressure difference; l is the effective channel length; ρ is the density of water.

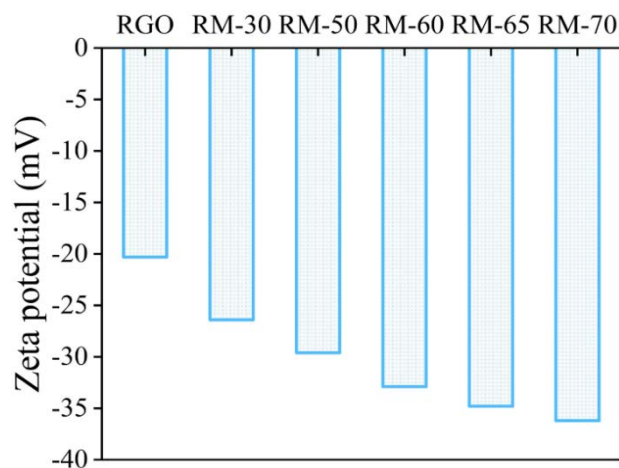


Fig. S8 Zeta potentials of RGO, RM-30, RM-50, RM-60, RM-65 and RM-70 membranes.

Membrane Cathode Potential Test

The test system was a three-electrode system (working electrode (cathode): RGO-MXene membrane, counter electrode (anode): platinum plate, reference electrode: Ag/AgCl electrode). The distance between the working electrode and the counter electrode was 1 cm, and the electrolyte was a 5 mM NaCl solution. The negative and positive electrodes of the DC stabilized power supply (WYJ-0-15V/5A, Shanjie Electric Technology Co., Ltd., Shanghai, China) were connected to the working electrode and the counter electrode, respectively. A certain external voltage was applied to the system through a DC stabilized power supply, and the open circuit voltage of the system was tested with an electrochemical workstation (CHI660, Chenhua Instrument Co., Ltd., Shanghai, China). The test time for each voltage was 200 s.

Cyclic voltammetry curve test

The test system was a three-electrode system (working electrode (cathode): RGO-MXene membrane, counter electrode (anode): platinum plate, reference electrode: Ag/AgCl electrode). The tested membrane area was 1 cm². The electrolyte was a 5 mM NaCl solution. The sweep range was 0 V to -2.0 V and the sweep rate was 10 mV/s.

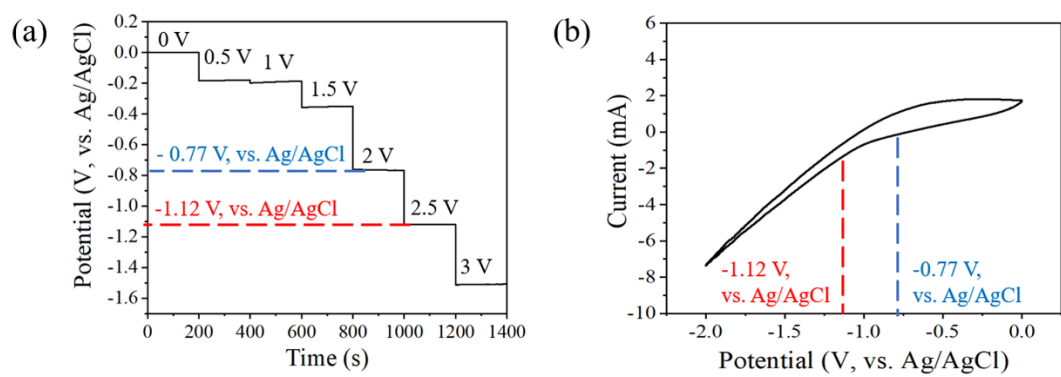


Fig. S9 (a) Membrane cathode potentials of RM-65 membrane under different voltages; (b) Cyclic voltammetry curve of RM-65 membrane.

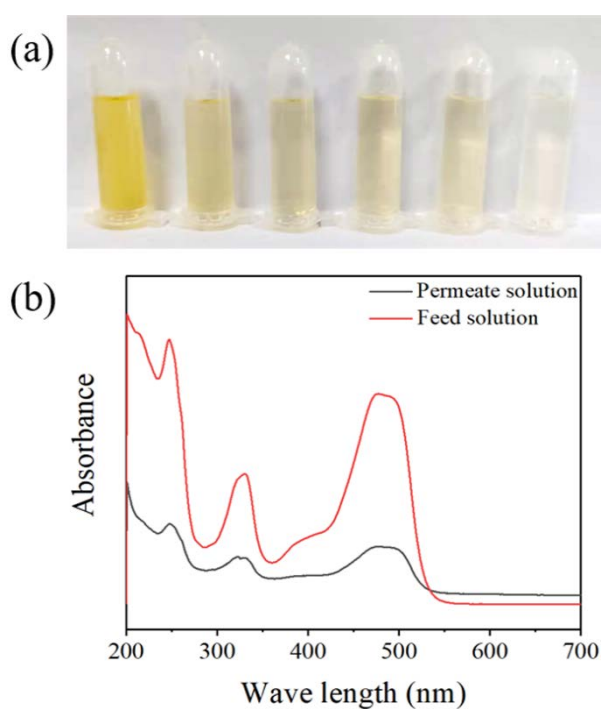


Fig. S10 (a) Digital photo of OG solutions. From left to right: the feed solution, the permeate solutions under voltages of 0 V, 0.5 V, 1.0 V, 1.5 V and 2.0 V, respectively; (b) UV absorption spectra of OG feed solution and permeate solution at 2.0 V.

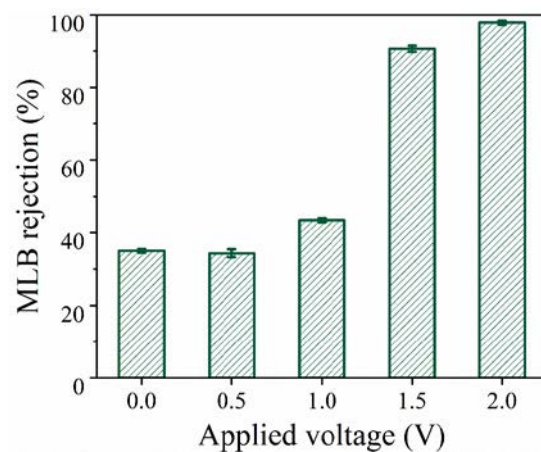


Fig. S11 Rejection rates of RM-65 membrane for MLB under different voltages (MLB concentration: 20 mg/L; pressure: 1 bar).

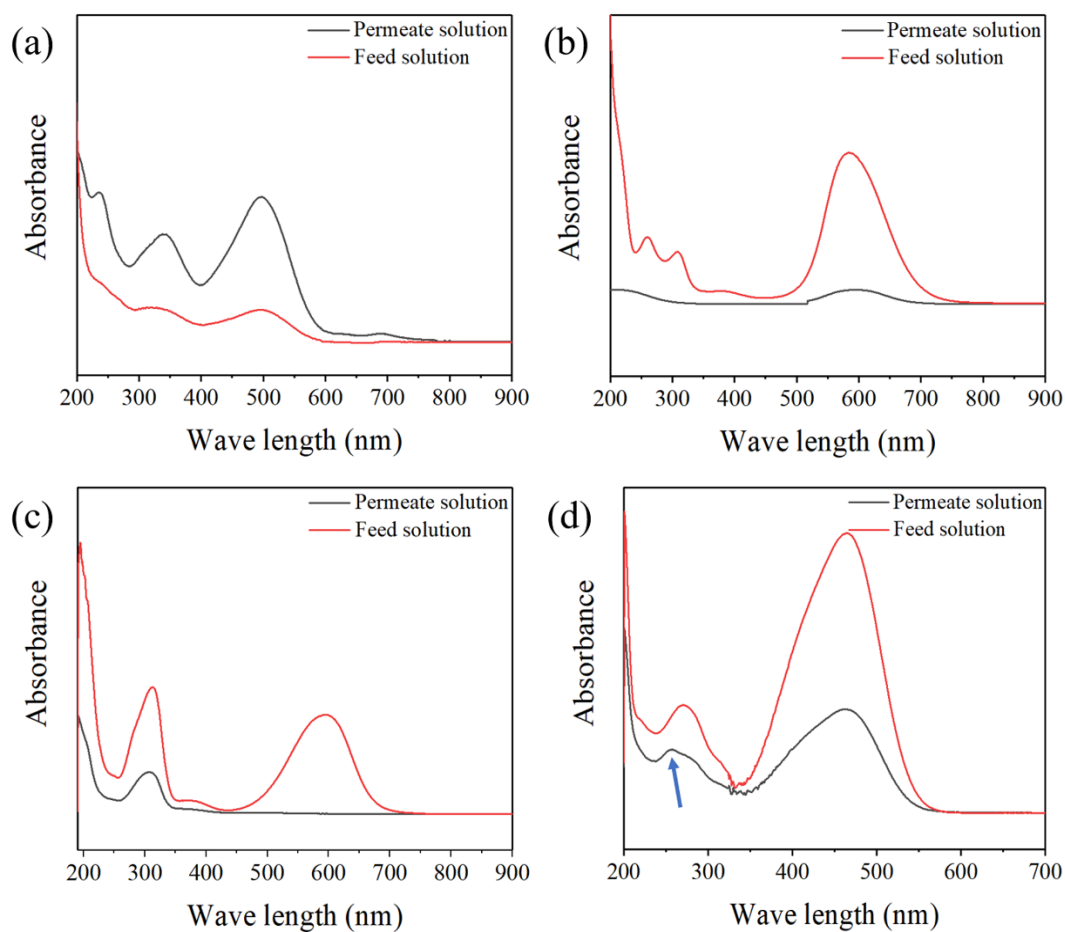


Fig. S12 UV absorption spectra of the feed solutions and the permeate solutions at 2.0 V: (a) CR; (b) CBB; (c) MB; (d) MO.

References

Nair R R, Wu H A, Jayaram P N, Grigorieva I V, Geim A K (2012). Unimpeded permeation of water through helium-leak-tight graphene-based membranes. *Science*, 335(6067): 442–444

Xu K, Ji X, Zhang B, Chen C, Ruan Y J, Miao L, Jiang J J (2016). Charging/discharging dynamics in two-dimensional titanium carbide (MXene) slit nanopore: insights from molecular dynamic study. *Electrochimica Acta*, 196: 75–83

Xu K, Lin Z, Merlet C, Taberna P L, Miao L, Jiang J, Simon P (2018). Tracking ionic rearrangements and interpreting dynamic volumetric changes in two-dimensional metal carbide supercapacitors: a molecular dynamics simulation study. *ChemSusChem*, 11(12): 1892–1899